Selective Synthesis and Coating of ZnO Nanomaterials

Jong-Soo Lee*, Myungil Kang*, Kwangsue Park*, Byungdon Min*, Joowon Hwang*, Kihyun Keem* and Sangsig Kim*

Abstract - Three different ZnO nanomaterials (nanobelts, nanorods, and nanowires) were synthesized at 1380 C from ball-milled ZnO powders by a thermal evaporation procedure with an argon carrier gas without any catalysts. Transmission electron microscopy (TEM) revealed that the ZnO nanobelts are single crystalline with the growth direction perpendicular to the (010) lattice plane, and that the ZnO nanorods and nanowires are single crystalline with the growth directions perpendicular to the (001) and (110) lattice planes, respectively. In cathodoluminescence (CL), the energy position of the near band-edge (NBE) peak is 3.280 eV for the 100-, 250-, and 500-nm thick nanobelts, 3.262 eV for the 100- and 250-nm thick nanorods, and 3.237 eV for the 500-nm thick nanorods. The synthesized ZnO nanorods were coated conformally with aluminum oxide (Al_2O_3) material by atomic layer deposition (ALD). Al_2O_3films were then deposited on these ZnO nanorods by ALD at a substrate temperature of 300 C using trimethylaluminum (TMA) and distilled water (H_2O). Transmission electron microscopy (TEM) images of the deposited ZnO nanorods revealed that 40nm-thick Al_2O_3 cylindrical shells surround the ZnO nanorods.

Keywords: ZnO nanomaterials, atomic layer deposition (ALD), selective synthesis

1. Introduction

Wide-gap compound semiconductors have highly potential applications for optoelectronic devices, in particular, emitting blue light. Direct-gap ZnO semiconducting material (Eg=3.37 eV at room temperature) is one of the attractive candidates for highly efficient optical devices operating at room temperature, since excitons formed in this material have a high binding energy of 60 meV[1-3], compared with other semiconducting materials (for instance, exciton binding energy is 22 meV for ZnSe, and 25 meV for GaN)[4,5]. Such a high exciton binding energy disables the role of phonons at room temperature since this binding energy is 2.4 larger than the effective thermal energy. For this reason, ZnO material emits efficient exciton emissions at high temperatures up to 550 K under low excitation energy[6].

The synthesis of nanostructured semiconducting materials has become an important research issue since the notable discovery of graphitic nanotubes[7]. Compound semiconducting nanomaterials including GaN[8,9], GaP[10], InP[11], ZnO[12,13], and Ga_2O_3[14] have been developed for the fabrication of nanooptoelectronic devices. In particular, the nanomaterials of metal-oxide-related semiconductors such as ZnO and Ga_2O_3 have been a matter of interest due to their excellent crystalline quality, chemical stability, thermal stability, and wide bandgap.

Recently, to realize these devices utilizing nanorods, the protection of the nanorods from contamination and from oxidation has become of crucial importance[13, 14]. Conformal coating of nanorods is required to retain their optical and electrical properties. Moreover, the three dimensional geometry of nanorods requires a high degree of control of the protecting layers [15, 16]. Atomic layer deposition (ALD) is one of the adequate techniques satisfying these requirements because of its nature of surface controlled process, such as atomic layer control, thickness controlled by the number of reaction steps and perfect control of growth rate. ALD is expected to be the ideal candidate of powerful growth methods for achieving conformal protecting layers.

This paper presents the structural and optical properties of three different nanostructured ZnO materials (nanowires, nanobelts, and nanorods) synthesized from the thermal evaporation of ball-milled ZnO powders, and shows the probability of applications for nano-electric and optical devices.

A comparison of products obtained from ZnO nanomaterials is first made by scanning electron microscopy (SEM), and the structural and optical properties of the synthesized nanomaterials are characterized by transmission electron microscopy (TEM), selected-area electron diffraction

* Dept. of Electrical Engineering, Korea Univerity, Korea (jsys0302@korea.ac.kr, nicekmi@korea.ac.kr, kwangsue@keti.re.kr, mbd7804@korea.ac.kr, mars21c@korea.ac.kr, blast79@korea.ac.kr, sangsig@korea.ac.kr)

Received September 30, 2002 ; Accepted December 28, 2002

(SAED), and cathodoluminescence (CL). The chemical components and structural properties of the deposited Al_2O_3 films were also investigated by energy-dispersive X-ray (EDX) spectroscopy and TEM.

2. Experimetal procedure

ZnO powders (-200 mesh) were used for synthesizing the nanomaterials under study. The ZnO powders were first ground for 20 hours in the mechanical ball mill system using a steel vial with 100 stainless steel balls, in which the mixture ratio of steal balls and ZnO powders was 15:1 in weight percents. An alumina boat containing the ball-milled ZnO powders was then loaded into the center of a horizontal alumina tube and 5×5 mm sized Si substrates were put at three different places in the tube (Fig. 1). The thermal evaporation of the ball-milled ZnO powders was performed at 1380℃ for 3 hours with an argon flow rate of 500 standard cubic centimeters per minute (sccm) under a constant furnace chamber pressure of 0.5 atm.

Al_2O_3 films were grown on the synthesized ZnO nanorods at a temperature of 300℃ by using the ALD technique. Trimethylaluminum (TMA) and distilled water were utilized as the precursors for the films. The process pressure was 280 and 250 mTorr for the dosing of chemical precursors and the Ar purging, respectively. The ALD method is a self-regulating process, so the precursor elements must be alternately dosed to the substrate. We choose this dosing time to be 2 sec, and purging time 20 sec. The one cycle for the growth of Al_2O_3 films is composed of TMA dosing, Ar purging, H_2O dosing and Ar purging, and the times of each are 2, 20, 2 and 20 sec. We have carried out 200 cycles to deposit Al_2O_3 films on ZnO nanorods. The thickness of Al_2O_3 films after 200 cycles processing is 40 nm.

The as-synthesized products were characterized by X-ray diffractometer diffraction (RIGAKU, D/MAX-IIA), field emission scanning electron microscope (HITACHI, S-4700), and transmission electron microscopy (JEOL, JEM 3000F) for the analysis of the microstructure. Room-temperature CL(monoCL2, Gatan) was performed at an acceleration voltage of 5kV.

3. Results and discussion

Fig. 2 shows the scanning electron microscopy (SEM) images of nanomaterials synthesized in three different zones in the furnace tube described schematically in Fig. 1. The temperature ranges of the three zones labeled in A, B, and C are 1030~900, 700~650, and 450~350℃, respectively. A comparison of the three SEM images illustrates that morphologies of three nanomaterials synthesized at different substrate temperatures are distinctively different from each other. A SEM image of Fig. 2(a) exhibits that the nanomaterials synthesized in the A zone are mixtures of nanobelts and nanorods; nanomaterials having a rectangular cross section are named nanobelts, and nanomaterials, and those having a hexagonal cross section are named nanorods(see the sinsert of Fig. 2(b)).

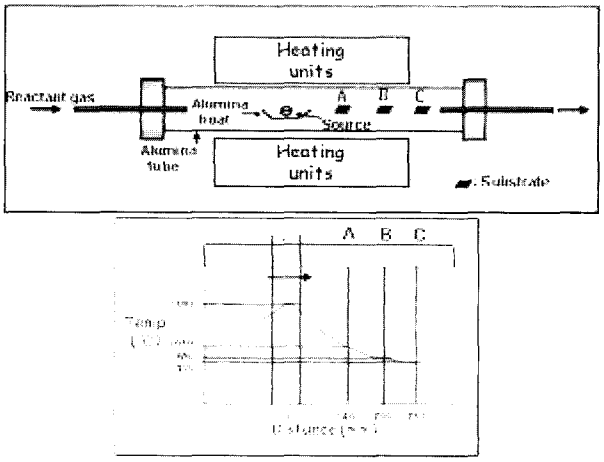

Fig. 1 Schematic illustration of the apparatus used in this work and the different temperature zones in the furnace tube.

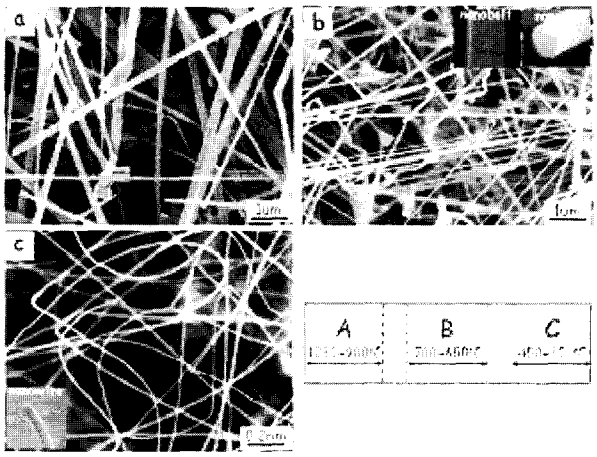

Fig. 2 SEM images of the ZnO nanomaterials grown in (a) A zone (1030~900℃), (b) B zone (700~650℃), and (c) C zone (450~350℃).

The nanobelts and nanorods synthesized in the A (1030~900℃) zone are in the range of several hundred nanometers to several hundred micrometers in width or in diameter. The SEM image of Fig. 2(b) reveals that the nanomaterials synthesized in the B (700~650℃) zone are also mixtures of nanobelts and nanorods, but that their sizes are in the range of 70 to 300 nm. In contrast, the SEM image of Fig. 2(c) shows that the nanomaterials syn-

thesized in the C (450~350℃) zone are nanowires; nanomaterials having a circular cross section are named nanowires(see the insert of Fig. 2(c)). The nanowires are in the range of 15 to 40 nm in diameter and in the range of 10 to 70 ㎛ in length; their diameters and lengths are very uniform, compared with the nanobelts and nanorods.

Fig. 3 shows the X-ray diffraction (XRD) patterns of starting ZnO powders, ball-milled ZnO powders, the nanobelts and nanorods (Fig. 2(b)) obtained from the thermal evaporation of the starting ZnO powders, and the nanowires(Fig. 2(c)) obtained from the thermal evaporation of the ball-milled ZnO powders; all the XRD patterns are normalized. The XRD pattern of the starting ZnO powders (Fig. 3(a)) is indexed to a wurtzite hexagonal structure of ZnO material with lattice constants of a=3.250℃ and c=5.205℃. For the ball-milled ZnO powders, XRD peaks are diminished in intensity and broadened in line width, compared with the starting ZnO powders. The XRD patterns of nanobelts, nanorods (Fig. 3(c)), and nanowires (Fig. 3(d)) are identical to that of the starting ZnO powders, so these products are identified to be crystalline ZnO materials.

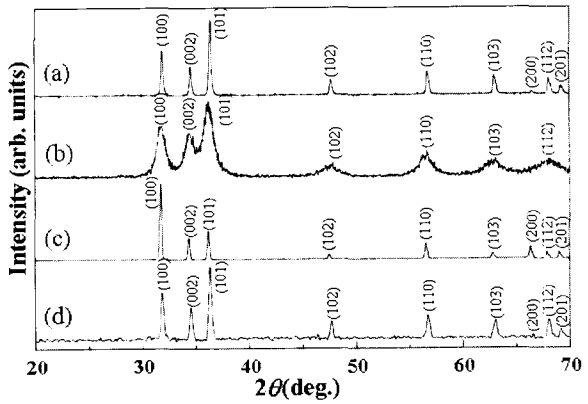

Fig. 3 XRD patterns of (a) starting ZnO powders, (b) ball-milled ZnO powders, (c) white colored products obtained from thermal evaporation of the starting ZnO powders, and (d) light-gray colored products obtained from thermal evaporation of the ball-milled ZnO powders.

The SEM images in Fig. 4 exhibit the side view of the nanomaterials grown on a Si substrate in the B zone and C zone. Fig. 4(a) shows that the nanobelts and nanorods are grown not from the Si substrate but from a thick layer of ZnO polycrystalline material on the top of the Si substrate, indicating that the thick layer is formed before the formation of the nanowires(Fig. 4(b)). These observations imply that the XRD pattern of the materials grown on a Si substrate in the B zone and C zone come not only from the nanomaterials but also from the thick layer. SEM images of the materials grown on Si substrates in the A and C zones also show the presence of the thick layers of ZnO polycrystalline material on the top of Si substrates. Both the nanomaterials (nanobelts, nanorods, and nanowires) and the thick layer may be ZnO materials, since no other peaks but the peaks related to the ZnO hexagonal phase are seen in the XRD patterns. Nevertheless, a possibility that the nanobelts, nanorods, and nanowires are not ZnO material is still not ruled out at this stage.

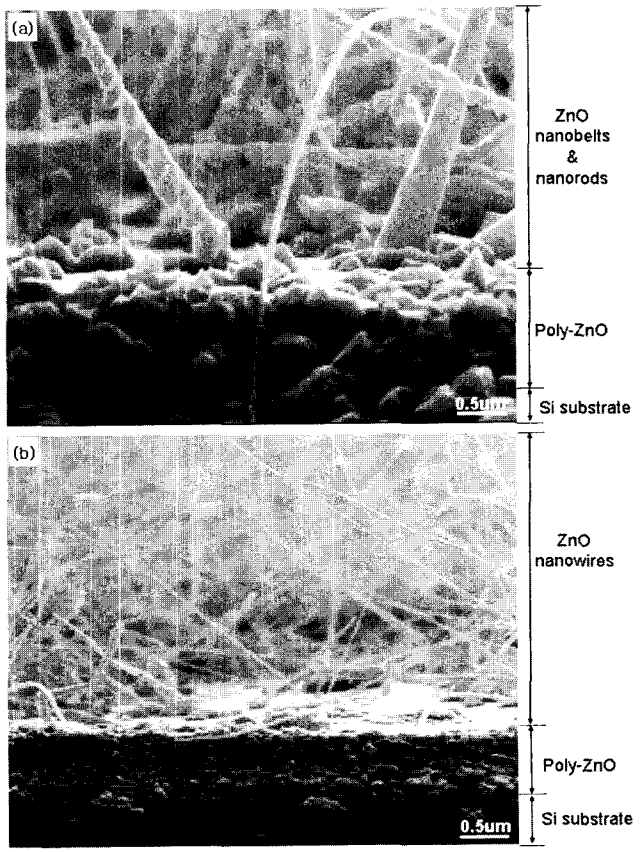

Fig. 4 The side view image of the materials grown on a Si substrate in the B zone(a), and C zone(b)

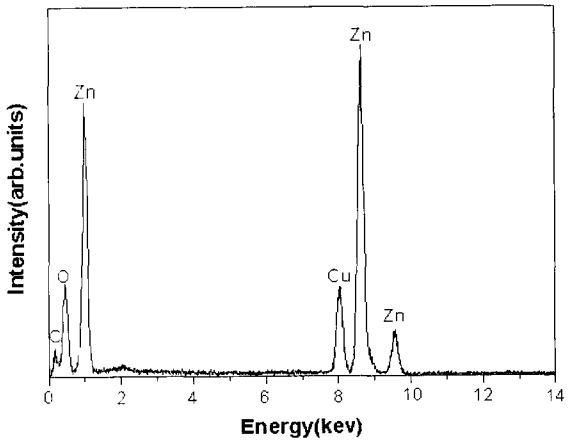

Fig. 5 Energy dispersive X-ray(EDX) spectrum of the nanomaterials.

A representative EDX spectrum of the nanomaterials (nanobelts, nanorods, and nanowires) is depicted in Fig. 5. Only the peaks associated with Zn and O atoms are seen in this EDX spectrum (the Cu-related peak in the spectrum comes from the Cu grids), leading to the obvious fact that the nanobelts, nanorods, and nanowires are indeed ZnO material.

Fig. 6 shows transmission electron microscopy (TEM) images of three selected nanomaterials : (nanobelt (a), nanorod (b), and nanowire (c)) the nanobelt and nanorod are selected from the nanomaterials synthesized in the B zone, and the nanowire is selected from the nanomaterials synthesized in the C zone. The insets of Figs. 6(a), 6(b) and 6(c) show three representative selected-area electron diffraction (SAED) patterns taken from these nanomaterials. In the SAED patterns, the direction of the zone axe is indexed to be the [100] lattice direction for the nanobelt (Fig. 6(a)), the [100] lattice direction for the nanorod (Fig. 6(b)), and the [110] lattice direction for the nanowire (Fig. 6(c)). The SAED reveals that the direction of the growth is perpendicular to the (010) lattice planes for the nanobelt (Fig. 6(a)), to the (001) lattice planes for the nanorod (Fig. 6(b)), and to the (110) lattice planes for the nanowire (Fig. 6(c)). On the basis of the TEM, SAED, and SEM analyses, the orientations of hexagonal lattice units in the nanobelts, nanorods, and nanowires may be determined. The determined orientations of hexagonal lattice units in regards to the growth directions of three different nanostructured ZnO materials are depicted in Fig. 7 in the hexagonal lattice units ; the hatched planes Fig. 7(a), Fig. 7(b), and Fig. 7(c) correspond to the lattice planes perpendicular to the zone axes in the insets Fig. 6 (a), Fig. 6 (b), and Fig. 6, respectively.

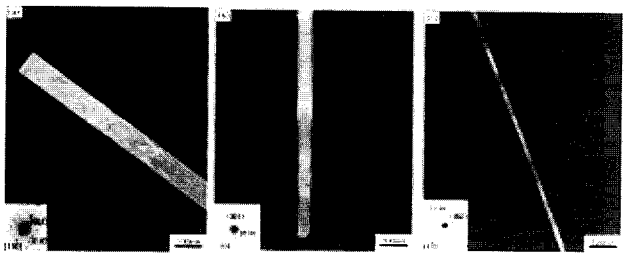

Fig. 6 TEM bright field images and their associated SAED patterns of a selected nanobelt(a), a selected nanorod(b), and a selected nanowire(c).

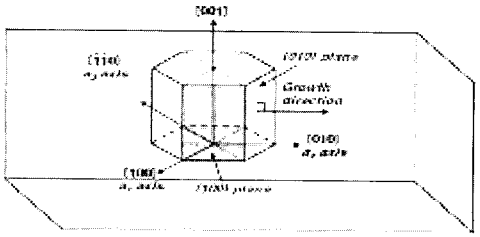

(a)

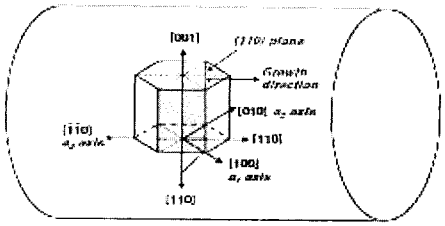

(b)

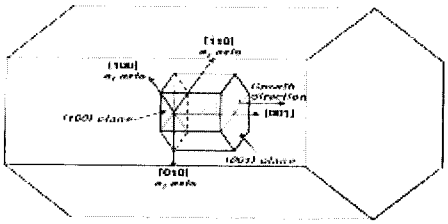

(c)

Fig. 7 The configurations of hexagonal lattice units in regards to the growth directions of the nanobelt(a), nanorod(b), and nanowire(c).

Fig. 8 exhibits size-selective CL spectra for six single nanobelts and nanorods selected from the nanomaterials synthesized in the B zone. The energy position of the near band-edge (NBE) peak is the same (3.280eV) for the 100-,

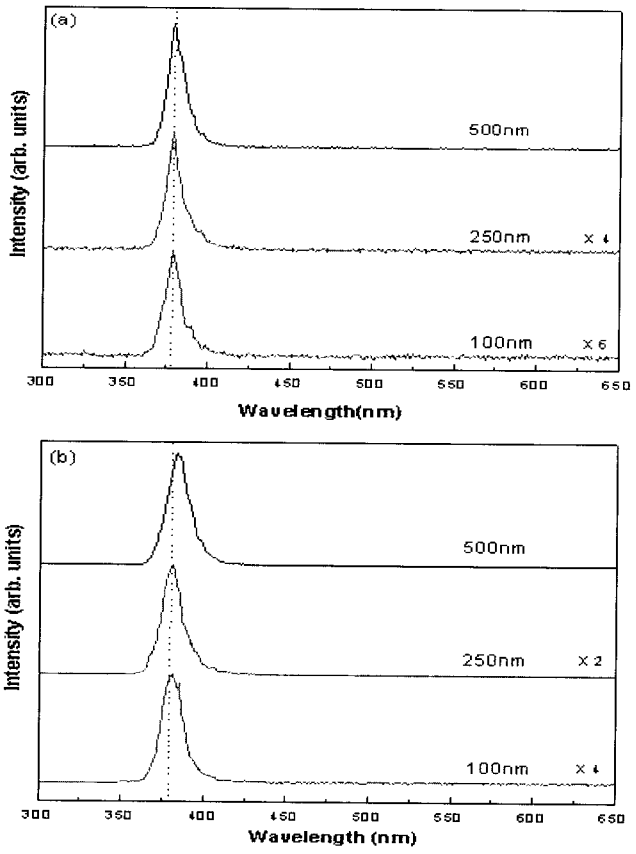

Fig. 8 The room temperature(300K) CL spectra of the ZnO nanobelts(a) and nanorods(b) selected from the nanomaterials synthesized in the B zone.

250-, and 500-nm thick nanobelts. For the nanorod, the energy position of the NBE peak is the same (3.262eV) for the 100 -and 250-nm thicknesses, but the energy position of the 500-nm thickness is 3.237 eV. Note that the NBE emission peaks are responsible for the recombination of free excitons. As the energy position of the NBE peak follows the bandgap, the bandgap of the nanobelts is independent of their size in the size range of 100 nm to 500nm, but the bandgap of the nanorod is not independent. In this size range, the bandgap depends not on the quantum confinement but on strain experienced entirely by nanomaterials[17]. Thus, the 500-nm thick nanorod may be experienced by tensile strain, compared with the other 100- and 250-nm thick nanorods.

The size-selective SEM and CL images of the nanobelts and nanorods were shown in Figs. 9 and 10, respectively.

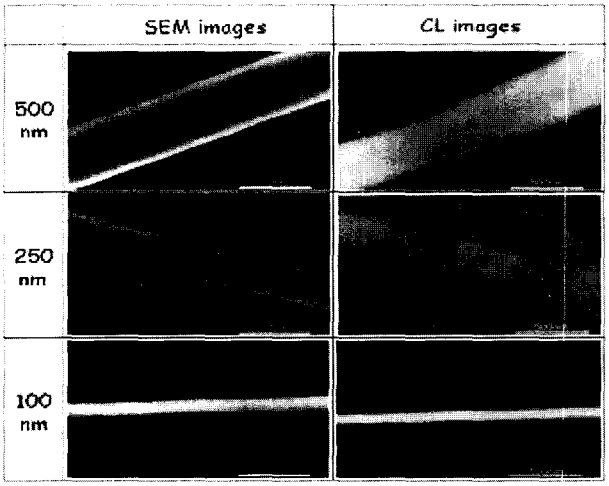

Fig. 9 The SEM images and CL images of 100- and 250-, and 500-nm thick ZnO nanobelts selected from the nanomaterials synthesized in the B zone.

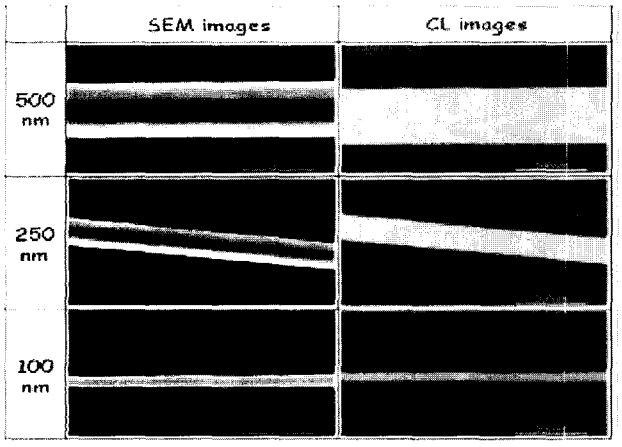

Fig. 10 The SEM images and CL images of 100- and 250-, and 500-nm thick ZnO nanorods selected from the nanomaterials synthesized in the B zone.

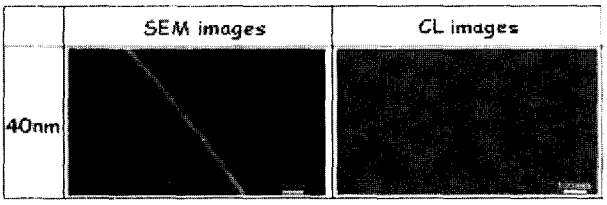

Fig. 11 The SEM image and CL image of a 40nm diameter ZnO nanowires synthesized in the C zone.

The CL images were each detected at the NBE peak positions of the corresponding CL spectra shown in Fig. 11. The CL images reveal that all the regions of the nanobelts and nanorods emit the NBE emission homogeneously; they do not show any dead spots that can not emit the NBE emission. However, the CL detection of the single nanowire(Fig. 11) selected from the nanomaterials synthesized in the C zone was a failure due to the weakness of the CL signal.

Fig. 12(a) is a TEM image of a selected ZnO nanorod deposited with Al_2O_3 materials by ALD. The TEM image illustrates that the cylindrical Al_2O_3 shell with the cap surrounds the ZnO nanorod. The Al_2O_3 shell is 40 nm in thickness; its thickness is quite uniform along the nanorod. The ZnO nanorod is coated conformally with Al_2O_3 material by ALD. Fig. 12(b) and Fig. 12(c) show the EDX spectra taken for the central and edge parts (marked by A and B,

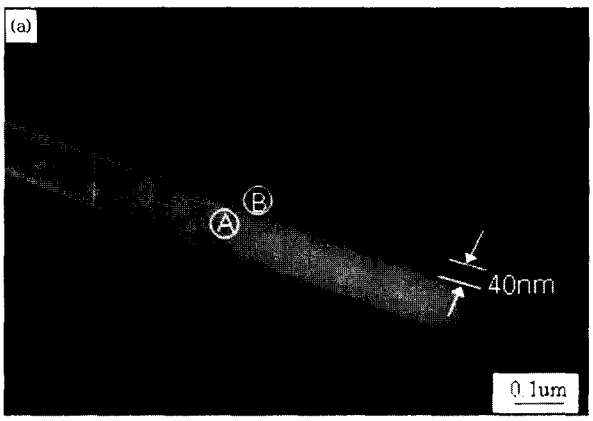

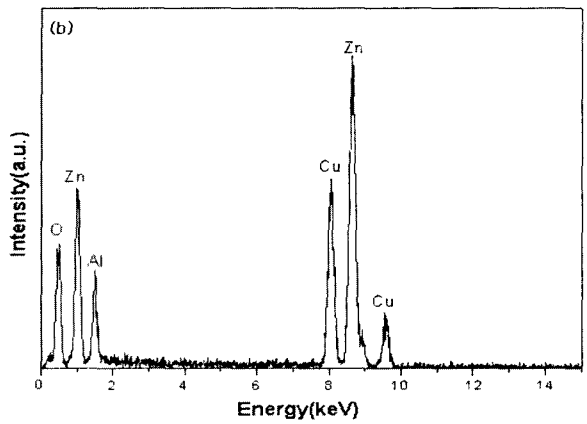

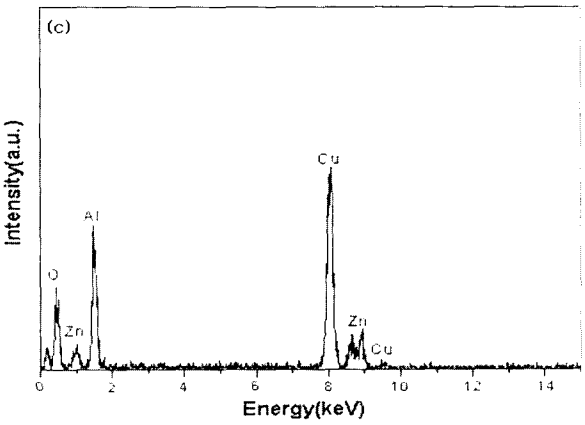

Fig. 12 The TEM image (a) of the Al_2O_3-deposited ZnO nanorod. The central part (A) is the ZnO nanorod and the outer part (B) is the deposited Al_2O_3 film. The EDX spectrum (b) taken for its central part, and the EDX spectrum (c) taken for its outer part.

respectively, in Fig.12(a)) of the coated ZnO nanorod. The EDX spectrum taken for its edge part exhibits that the Al-related peak is stronger in intensity than the Zn-related peak, which indicates that the deposited part is indeed Al_2O_3. Additionally, an Al_2O_3 film was deposited on a plain Si substrate by ALD under the same deposition condition as on the nanorods in this study. In a Fourier transform infrared (FTIR) spectrum taken for this Al_2O_3 film grown on a Si substrate (not shown here), a broad absorption band associated with amorphous Al_2O_3 was observed. It is well known that the crystal structure and chemical components of the layers deposited by ALD are independent of the substrate [18]. Hence, we have concluded that the coating material of the ZnO nanorod is amorphous Al_2O_3.

4. Conclusion

ZnO nanobelts, nanorods, and nanowires were synthesized at three different substrate temperatures from the thermal evaporation of ball-milled ZnO powders at 1380 ℃. SEM revealed that the nanobelts and nanorods synthesized in the substrate temperature (1030~900 ℃) zone are in the range of several hundred nanometers to several hundred micrometers in width or in diameter, that nanobelts and nanorods synthesized in the substrate temperature (700~650 ℃) zone are in the range of 70 to 300 nm in width or in diameter, and that the nanowires synthesized in the substrate temperature (450~350 ℃) zone are in the range of 15 to 40 nm in diameter. TEM revealed that the ZnO nanobelts, nanorods, and nanowires are single crystalline with the growth direction perpendicular to the (010), (001) and (110) lattice planes, respectively. In addition, the energy position of the near band-edge (NBE) peak is 3.280 eV for the 100-, 250-, and 500-nm thick nanobelts, 3.262 eV for the 100- and 250-nm thick nanorods, and 3.237 eV for the 500-nm thick nanorods. The CL images reveal that all the regions of the the nanobelts and nanorods emit the NBE emission homogeneously.

After the synthesis of ZnO nanorods from ball-milled ZnO powders by a thermal evaporation procedure, conformal Al_2O_3 layers were successfully deposited on the ZnO nanorods by ALD. TEM images of the deposited ZnO nanorods revealed that 40nm-thick Al_2O_3 cylindrical shells surround the ZnO nanorods.We suggested here that the coated layers on the nanorods might be an indicator of the growth rate of the ALD system. Furthermore, conformally deposited Al_2O_3 layers on nanorods may play important roles as protecting layers and gate layers. Hence, the results in this study may fasten the realization of the nanorod devices.

Acknowledgements

This work was supported by the Korean Ministry of Science and Technology as a part of the '02 Nuclear R&D Program, Grant No. 1999-2-302-017-5 and Grant No. R01-2002-000-0(2002) from the Basic Research Program of the Korea Science & Engineering Foundation, and the '02 Hanbit Project of the Korea Basic Science Institute.

References

[1] J. M. Hvam, *Phys. Rev. B* 4 (1971) 4459.
[2] C. Klingshirn, *Phys. Status Solidi B* 71 (1975) 547.
[3] R. F. Service, *Science* 276 (1997) 895.
[4] Michael H. Huang, Samuel Mao, Henning Feick, Haoquan Yan, Yiying Wu, Hannes Kind, Eicke Weber, Richard Russo, Peidong Yang, *Science*, 292 (2001) 1897.
[5] Y. F. Chen, D. M. Bagnall, H. Koh, K. Park, K. Hiraga, Z. Zhu, T. Yao, *J. Appl. Phys.* 84 (1998) 3912.
[6] D. M. bagnall, Y. F. Chen, Z. Zhu, T. Yao, M. Y. Shen, T. Goto, *Appl. Phys. Lett.* 73 (1998) 1038.
[7] N. Hamada, S. Sawada, A. Oshiyama, *Phys. Rev. Lett.* 68 (1992) 1579.
[8] W. Han, S. Fan, Q. Li, Y. Hu: *Science* 277 (1997) 1287.
[9] J. Y. Li, X. L. Chen, Z. Y. Qiao, Y. G. Cao, Y. C. Lan: *J. Cryst. Growth* 213 (2000) 408.
[10] W.S. Shi, Y. F. Zheng, N. Wang, C. S. Lee, S. T. Lee, *Chem. Phys. Lett.*, 345 (2001) 377.
[11] Xiangfeng Duan, Yu Huang, Yi Cui, Jianfang Wang, and Charies M. Lieber, *nature*, 409 (2001) 66.

[12] Z. W. Pan, Z. R. Dai, Z. L. Wang: *Science* 291 (2001) 1947.
[13] M. H. Huang, Y. Wu, H. Feick, N. Tran, E. Weber, P. Yang: *Adv. Mater.* 13 (2001) 113.
[14] H. Z. Zhang, Y. C. Kong, Y. Z. Wang, X. Du, Z. Bai, J. J. Wang, D. P. Yu, Y. Ding, Q. L. Hang, S. Q. Feng: *Solid State Commun.* 109 (1999) 677.
[15] A. W. Ott, J. W. Klaus, J. M. Johnson, and S. M.George, *Thin Solid Films* 292, (1997) 135
[16] Y. Nakagome, and K. Itoh, *IEICE Trans.* E-74, (1991) 799
[17] Kwangsue Park, Jong-Soo Lee, Man-Young Sung, Sangsig Kim, accepted *to Japanese Journal of applied physics*, (2002. 9)
[18] Y. Kim, S. M. Lee, C. S. Park, S, I, Lee, and M. Y. Lee, *Appl. Phys. Lett.* 71, (1997) 3604.

Jong-Soo Lee
He received his BS, MS and Ph. D. degrees in metallurgical engineering from Chonbuk National University, Korea, in 1994, 1996, and 1999, respectively. He is a Research Professor in the Department of Electrical Engineering, Korea University. Seoul, South Korea.
Tel: +82-2-3290-4785, Fax: +82-2-3290-3894

Myung-Il Kang
He received his BS degree in electronic materials engineering from Kwangwoon University, Korea, in 2002.
Currenty, he is a graduate student in the Department of Electrical Engineering in Korea University, Seoul, South Korea.
Tel: +82-2-3290-3898, Fax: +82-2-3290-3894

Kwangsue Park
He received his BS and MS degrees in physics and electrical engineering from Korea University, Korea, in 2000 and 2002, respectively. He is currently working as an Researcher in the NANO scale quantum devices Research Center, Korea Electronics Technology Institute, PyungTaek, South Korea
Tel: +82-31-6104-238, Fax: +82-31-6104-148

Byungdon Min
He received his BS, MS and Ph. D. degrees in physics from Korea University, Korea, in 1985, 1987 and 1998, respectively. He is a Research Professor in the Department of Electrical Engineering ,Korea University, Seoul, South Korea.
Tel: +82-2-3290-4785, Fax: +82-2-3290-3894

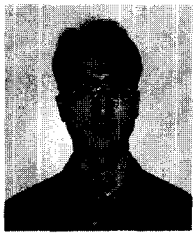

Joowon Hwang
He received his BS degree in electrical engineering from Konkuk university, Korea, in 2002. Currenty, he is a graduate student in the Department of Eelectrical Engineering in Korea University, Seoul, South Korea.
Tel: +82-2-3290-3909, Fax: +82-2-3290-3894

Kihyun Keem
He received his BS degree in electrical engineering from Korea University, Korea, in 2001. He is currently a MS candidate in Electrical Engineering, Korea University, Seoul, South Korea.
Tel: +82-2-3290-3898
Fax: +82-2-3290-3894

Sangsig Kim
He received his BS and MS degrees in physics from Korea University, Korea, in 1975, 1977 and 1981, respectively, and Ph. D in applied physics from Columbia University, USA, in 1996. He is a Professor in the Department of Electrical Engineering, Korea University, Seoul, South Korea.
Tel: +82-2-3290-3245, Fax: +82-2-3290-3894